



TotalControl

Advanced integrated supervisory and wind turbine control for optimal operation of large Wind Power Plants

Predictive control algorithms based on reduced-order physical models

D4.3

Delivery date: 15.03.2022

Lead beneficiary: DTU

Dissemination level: Public



This project has received funding from the European Union's Horizon 2020 Research and Innovation Programme under grant agreement No 725076.

Authors information:

Name	Organisation	Email
Alan Wai Hou Lio	DTU	wali@dtu.dk
Ishaan Sood	KU Leuven	ishaan.sood@kuleuven.be

Acknowledgements/Contributions:

Name	Name	Name
-------------	-------------	-------------

Document information:

Version	Date	Prepared by	Reviewed by	Approved by
1.0	30th May 2022	Alan Wai Hou Lio Ishaan Sood	Konstanze Kölle	

Definitions/abbreviations

MPC	Model predictive control
CFD	Computational fluid dynamics
TSO	Transmission system operator

EXECUTIVE SUMMARY

The first part of this study presents a model predictive control (MPC) for an active power control, in which the total wind farm power production is required to follow a power reference signal provided by the transmission system operator (TSO). Specifically, the proposed predictive control takes into account the wind flow predictions within a wind farm using a dynamic flow model. The dynamic flow model is developed based on Fuga, which is a linearized computational fluid dynamics (CFD) model. By the Taylors' frozen turbulence assumption, assuming the wake as a mass of air travelling downwind with a mean wind speed, the dynamic Fuga can model the wake propagating downstream with respect to changes in control variable, which is the turbine power coefficient in this case, and changes in wake-free ambient wind speeds. The dynamic Fuga model can provide fast, accurate and time-varying wind flow predictions within a wind farm, which is essential for model predictive control. The proposed MPC algorithm is then evaluated in a wind farm with three turbines in a row, showing remarkable tracking performance in cases where the wind speed is sufficiently high to produce the required power by the TSO. In a low wind speed case where the power available in the wind is not sufficient to meet the power requirement by the TSO, the MPC managed to track the power reference by the TSO as close as possible.

The second part of this study presents a closed loop methodology for wind farm power maximisation. By steering the wakes of upstream turbines away from downstream turbines through yaw control, the total power produced by a wind farm can be increased. The closed loop methodology consists of an analytical wake model coupled with a high fidelity Large Eddy Simulations (LES) suite. Through feedback quasi-static control, measurements are taken from the LES domain which serve as inputs for the wake model, which in turn is used as a state model to optimize the farm performance. The framework also consists of online calibration to improve model predictions for different wind directions and atmospheric conditions. Comparisons are made against open-loop control, with previous power maximisation simulations with the TotalControl Reference Wind Power Plant (TC RWP) serving as a reference.

1 MODEL PREDICTIVE CONTROL BASED ON FUGA

1.1 Introduction

Placing wind turbines in wind farms closely can reduce the use of lands and costs of installation, operations and maintenance. However, when wind turbines are installed in close proximity, the downstream turbines are likely to be subject to the wake generated by the upstream turbine. These complex interactions cause a loss in wind velocity (wake velocity deficit) and increase the turbulence (added turbulence) for the downstream turbine, leading to decreased power capture and accelerated structural degradation. These challenges motivate the research of wind farm control, coordinating the operation of the turbines to mitigate the wake effect.

There are three main control objectives in wind farm control: (i) to increase the energy yield; (ii) to reduce structural loads of turbines; and (iii) to provide ancillary service to the electrical grid. One of the ancillary service examples to improve the grid reliability is secondary frequency regulation, in which the wind farm tracks the power reference provided by transmission system operators (TSO) [1]. The task is also known as power tracking [2] or active power control [1]. The power tracking can stabilise the grid frequency or provide a power reserve allowing for a fast response to changes in demand from the grid. Since the power reference signal is below the maximum available power in the wind, there exist a number of solutions for the tracking problem. Thus, besides minimising the tracking error, additional objectives can be considered in the wind farm control, for example, to alleviate the turbine structural loads, increase the wind farm available power/power reserve, minimise the rate of change in power commands to the turbine.

One of the earliest studies in wind farm power tracking are conducted by [3], where the wind farm controller distributes the turbine power set-points proportionally based on the available power at each turbine. This method is adopted by many later works (e.g. [4], [5]). Some studies investigated the possibility to provide ancillary service on the turbine level [1][6] [7] [8][9]. Later, unlike the earliest approach, a study by [10] proposed a wind farm controller that exploits the proportional-integral (PI) control structure. The tracking error between the power reference from the grid and power generation by the wind farm is directly fed back to the controller in order to compute the power set-point for each turbine. This method is then validated in a study by [11] on a scaled turbine in a wind tunnel. Some follow-up studies [12] [13] incorporate an additional PI loop to reduce turbine structural fatigue loads. These conventional control methods might result in multiple loops that require heavy tuning. Furthermore, multiple control objectives, constraints and advanced information cannot be incorporated into the design systematically.

Therefore, the development of model predictive control (MPC) for active power control problem is motivated, in which MPC can handle multiple control objectives, constraints and upcoming information. In general, MPC selects the predicted future control inputs based on the optimization of a performance criterion subject to the need for system predictions to satisfy constraint requirements. System predictions are obtained using a mathematical model of the system as well as measurements of the outputs at each sample. In the context of active power control, the models need to describe turbine dynamics and/or wind farm flow dynamics. Of many MPC strategies in active power control have been published in recent years, most can be grouped into two distinct classes, characterised by whether a wake model is incorporated in the MPC formulation.

The popular approach solves the power tracking problem using MPC with no wake model, where the controller is formulated solely based on turbine dynamics. The real-time measurement of turbine power outputs or wind speeds at turbines provides a feedback mechanism, ensuring the tracking error is minimised. One of the earliest studies using this approach is by [14], where a hierarchical wind farm controller that consists of two levels of controllers at different time-scale is developed for tracking the power reference. These controllers are formulated around a constant operating point/wind speed. A follow-up study [15] takes into account the turbine structural loads by minimising the variations in rotor thrust. Similarly, studies by [16, 17, 18] explored the

possibility of distributed MPC implementation on the active power control problem. Notice that all of these MPC wind farm controllers are validated in a simplified wind farm model [5]. Later, a study by [19] developed an MPC formulation based on an assumption that the wind speed at turbines is constant over the prediction horizon. The approach is validated in large-eddy simulation (LES). A follow-up study [2] extends the implementation to a stochastic framework. In [20], turbine structural loads are taken into account.

The assumption that the wind speeds at turbines are constant over the prediction horizon is valid as long as the horizon only covers a relatively short period of time (e.g. a few second). However, for a longer time horizon, there would exist mismatches between the model prediction and true system behaviour. Thus, control decisions based on an optimization of an inaccurate prediction could be poor. In a long time-scales (e.g. tens of seconds), turbines experience significant impact on each other through the wake interactions. Incorporating this strong coupling in the model is crucial for an effective MPC performance. Modelling of the dynamics of flow in a large-scale wind farm is computationally challenging. Developed engineering models such as Jensen-Park model and Frandsen wake models offer fast but steady-state wake predictions. A typical power reference signal could vary in a time-scale of a few seconds, for example, RegD [21]. Using these static models results in an MPC with slow sampling period in the order of minutes, which cannot respond to the fast changes in the power reference. For example, a study by [22] developed a distributed MPC based on a Jensen-Park and Gaussain wake model with a sample period of 52s and validated in FLORIS [23]. A 2D dynamic wake model WFSim is developed based on a 2D Navier Stokes equations [24]. Since the model is in a nonlinear descriptor state-space form, a study by [25] exploited the adjoint-based gradient method to find the optimal power set-point in the nonlinear framework. An execution time of 7 seconds for each time step is reported for a wind farm with six turbines in [26]. A study by [27] developed a dynamic flow model based on the static Frandsen wake model and used an MPC in [28]. The approach requires linearization around the turbine instantaneous wind speed, which might be inaccurate for a long prediction horizon.

Therefore, a computationally efficient MPC and wake model are needed for the active power control problem. In this work, we propose efficient model predictive control based on a dynamically propagated flow model. Specifically, the dynamic wake model is developed based on Fuga [29], a linearised computational fluid dynamics (CFD) Reynolds-averaged Navier-Stokes (RANS) wake model, which provides extremely fast static wake predictions. Similar to [30], the proposed dynamic flow model incorporates the time propagation of the control variable into Fuga and together with the turbine dynamics, a fast linear parameter-varying (LPV) model is formed. To solve the optimization problem with a LPV model, an efficient MPC is synthesized where the nonlinear problem can be solved rapidly by a series of quadratic programs at each time step.

1.2 Control-oriented modelling

This section presents the modelling of turbines and the dynamic Fuga model that describes the wind flow in a wind farm.

1.2.1 Turbine modelling

Considering a wind farm with N_T turbine, the electrical power P generated by the j -th turbine is given as follows:

$$P_j = \frac{1}{2} \rho \pi r^2 v_j^3 C_{p,j}(\lambda_j, \theta_j) \quad (1)$$

where $\rho, r \in \mathbb{R}$ are the air density and blade length whilst v_j are the wind speed at turbine j . The power coefficient, $C_{p,j}$ is a function of the pitch angle θ_j and tip-speed ratio $\lambda_j := \frac{\omega_j r}{v_j}$, where ω_j is the rotor speed. The turbine derating strategy has a large impact on the wake effect in a wind farm, thus resulting in different power and structural cost function. In the following section, the turbine controller and derating operation are discussed.

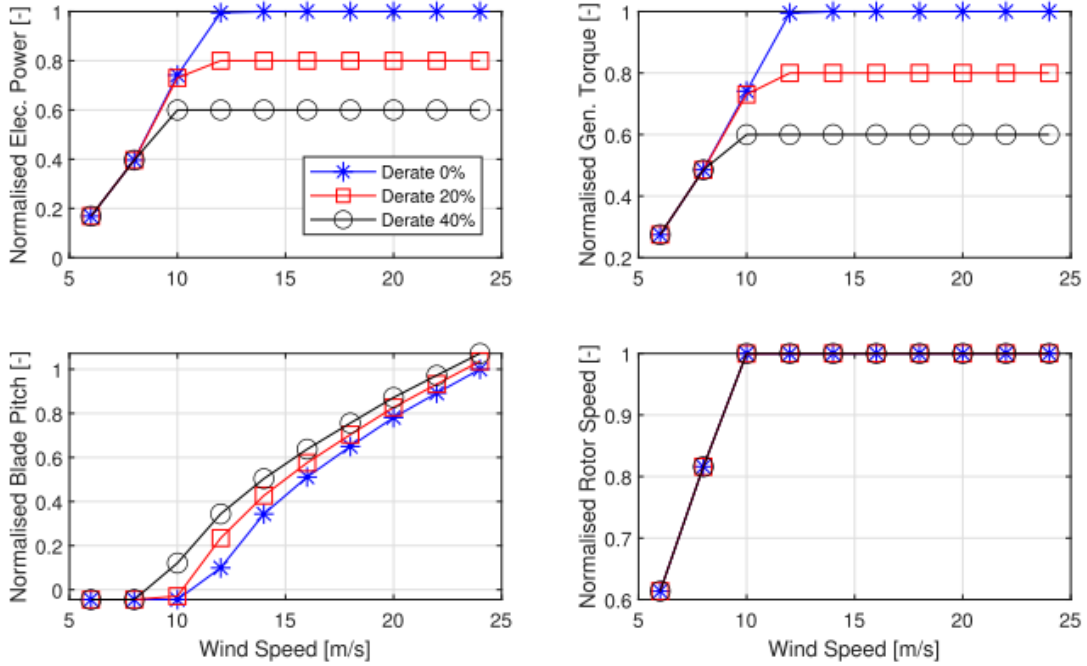


Figure 1: Normalised wind turbine mean electrical power, torque, blade pitch and rotor speed curves as a function of wind speed for different derating percentages [32].

1.2.2 Basic turbine controller

Basic wind turbine controllers typically consist of the generator torque and blade pitch controllers. The generator torque control law is defined as follows:

$$\tau_g(t) = \begin{cases} K_{\text{opt}}\omega(t)^2, & \text{if } \theta(t) \leq \theta_s, \\ \frac{P_{\text{rated}}}{\omega(t)}, & \text{if } \theta(t) \geq \theta_s, \end{cases} \quad (2a)$$

$$\tau_g(t) \in [\underline{\tau}_g, \bar{\tau}_g], \quad (2c)$$

The operating conditions are dependent on the switching parameter of the pitch angle θ_s . In below-rated wind condition (2a), the generator torque controller maximises the turbine power by tracking the optimal tip-speed ratio with the optimal gain $K_{\text{opt}} \in \mathbb{R}$, whilst in the above-rated wind condition (2b), the controller maintains the power at the rated value $P_{\text{rated}} \in \mathbb{R}$. The generator torque is constrained by the minimum and maximum limits denoted as $\underline{\tau}_g, \bar{\tau}_g \in \mathbb{R}$. For brevity, the aspects of how the controller (2) handles transitions around the start-up and the rated rotor speed are omitted from this paper and more details can be found in [31].

The blade pitch controller is typically designed as a gain-scheduled proportional-integral (PI) controller, defined as follows:

$$\theta(t) = f_{\text{PI}}(\omega(t) - \omega_{\text{rated}}), \quad \theta \in [\theta_{\min}, \theta_{\max}], \quad (3)$$

The PI control law $f_{\text{PI}} : \mathbb{R} \rightarrow \mathbb{R}$ drives the rotor speed to the rated value $\omega_{\text{rated}} \in \mathbb{R}$ and typically, it is gain-scheduled by the pitch angle (e.g. [31]), whilst the pitch angle is limited by $\theta_{\min}, \theta_{\max} \in \mathbb{R}$.

1.2.3 Down-regulation strategies

The power produced by a turbine is a product of the generator torque and the generator speed. Down-regulation can be achieved by either manipulating the generator torque or rotor speed set-point [6]. Therefore, a number of derating strategies exist in the literature [9]. This work considers torque-based down-regulation strategies, which is also known as Max-Omega strategy.

The torque-based strategy performs turbine down-regulation by changing the generator torque input solely. To implement the torque-based strategy, a new maximum torque limit $\bar{\tau}_{g,derated} \in \mathbb{R}$ is imposed on the generator torque in (2c), defined as follows:

$$\bar{\tau}_{g,derated} = \frac{P_{derated}}{\omega_{rated}} = \frac{\delta P_{rated}}{\omega_{rated}}, \quad (4)$$

where $P_{derated} \in \mathbb{R}$ denotes the derated power and the derating set-point δ is defined as a percentage of the rated turbine power. One of the benefits of such a strategy is that during power curtailments, the rotor speed is operating at rated and thus reserving the maximum amount of spinning energy for providing fast frequency response support to the grid [33]. As soon as the nominal rotor speed is reached, the blades are pitched towards feathering to reduce the power to the desired level. Figure 1 shows the steady-state turbine operational pitch angle and rotor speed, as well as the electrical power output and generator torque at different derating set-points.

1.2.4 Flow modelling

The wind speeds v_j experienced by downstream turbines in a wind farm are subject to complicated interactions. These wind speeds depend on the past control actions of the upstream turbines and the past free-stream wind speed v_∞ . Fast steady-state predictions can be obtained with static models such as Fuga [29]. To compute the turbine power output prediction within a time scale of one minute, static model prediction is not sufficient and it is crucial to incorporate the propagation effect of the control actions and ambient wind speeds.

Fuga is a linearized computational fluid dynamics (CFD) Reynolds-averaged Navier-Stokes (RANS) wake model, which is extremely fast to compute the stationary flow within a wind farm. The governing Navier-Stokes equations are consistently linearized using a perturbation expansion and subsequently retaining the first-order terms. Thus, mass and momentum conservations are both identically satisfied to first order; and the resulting flow fields are divergence free, as they should be for an assumed incompressible flow. The resulting equations are in turn conveniently formulated and solved in a mixed-spectral domain for efficiency reasons. The velocity perturbation around a single turbine in the physical domain is derived from Fourier components of the mixed-spectral solution using a fast inverse Fourier integral transform and stored in a system consisting of both general and turbine-specific look-up tables, which facilitates the extreme computational speed of the model prediction. Given the merit of being a linear model, Fuga can easily superimpose wakes from multiple upstream turbines to form the flow field further downstream. The Fuga model has been validated with full-scale measurements [34, 35].

The proposed dynamic Fuga model is a state-space model that consists of the static nonlinear mapping (Fuga) describing the steady-state flow prediction in a wind farm and a dynamic model that describes the propagation of control variables and wake-free wind speeds. The static mapping between thrust coefficients C_t and downstream wind speeds v provided by Fuga is defined as follows:

$$v_{\mathbf{x}} = f(v_\infty, \mathbf{C}_t) \quad (5)$$

where v_∞ denotes the upstream wake-free wind speed, $\mathbf{C}_t := [C_{t,1}, C_{t,2}, \dots]$ denotes the thrust coefficients of the upstream turbines and \mathbf{x} is the location of the observation point. Notice for the wind speed at a given turbine, it is only necessary to consider the upstream thrust coefficients. Given that a typical turbine considers the power set-point (derating signal) δ as an

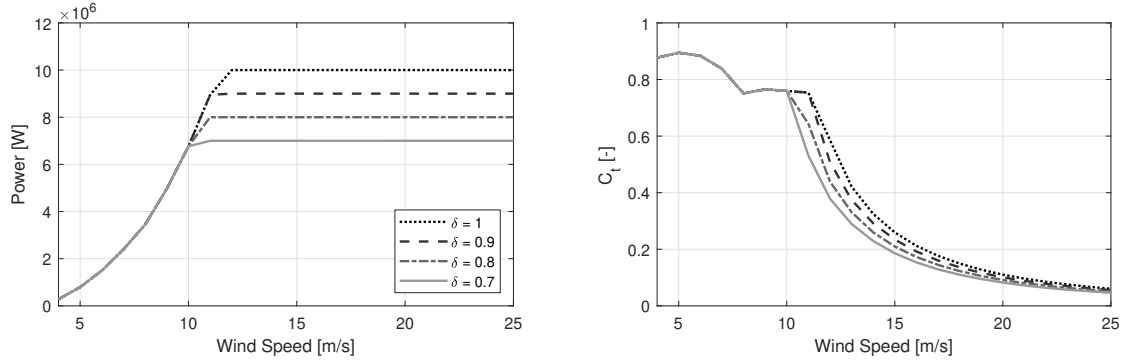


Figure 2: Simple turbine model in PyWake that describes the electrical power and thrust coefficient C_t in terms of derating level δ .

input, it is more convenient if (5) is a function of the power set-point. The relationship between power set-point and thrust coefficient is turbine-dependent. Figure 2 shows an example of the relationship of DTU10MW. The nonlinear turbine-dependent relationship can be represented as look-up tables

$$C_{t,j} = g(\delta_j, v_j) \quad (6)$$

An open-source framework for wind farm design, PyWake, can handle the Fuga wake model and the turbine relationship. Thus, the static Fuga model with an input space as the power set-point can be described as follows.

$$v_x = h(v_\infty, \delta) \quad (7)$$

where $\delta := [\delta_1, \delta_2, \dots]^T \in \mathbb{R}^{N_T}$ denotes a vector of derating signals of all turbines in a wind farm.

A dynamic wind flow is a function of the past and current turbine control actions and wake-free wind speeds. To incorporate the time propagation into the static model Fuga, a vector is defined to store the past power set-point and wake-free wind speeds v_{∞_k} , as follows:

$$\underline{\delta}(t) = [\delta(t - \Delta t), \delta(t - 2\Delta t), \dots, \delta(t - N_p \Delta t)], \quad (8)$$

$$\underline{v}_{\infty}(t) = [v_\infty(t - \Delta t), v_\infty(t - 2\Delta t), \dots, v_\infty(t - N_p \Delta t)], \quad (9)$$

where Δt is the sampling period and N_p is the number of observation points.

Figure 3 depicts the formulation of dynamic Fuga. The dynamic Fuga model relies on the concept of the Dynamic wake meandering (DWM) model [36], that shows the wake centre can be considered as a passive tracer which moves downstream with the mean wind speed. Therefore, at each given point downstream, the wind speed is defined by the past thrust coefficient of the upstream turbines and past wake-free wind speed. Let's take three turbines as an example in Figure 3. First, the stream-wise distance between observation points Δx needs to be defined and subsequently, the sampling period Δt of the model is determined by $\Delta x / \bar{v}_\infty$. Second, from the vectors of time-delayed input (8), the wind speeds at each observation point can be computed using the static model Fuga. Notice the wind speed evaluation can also be extended in the lateral direction.

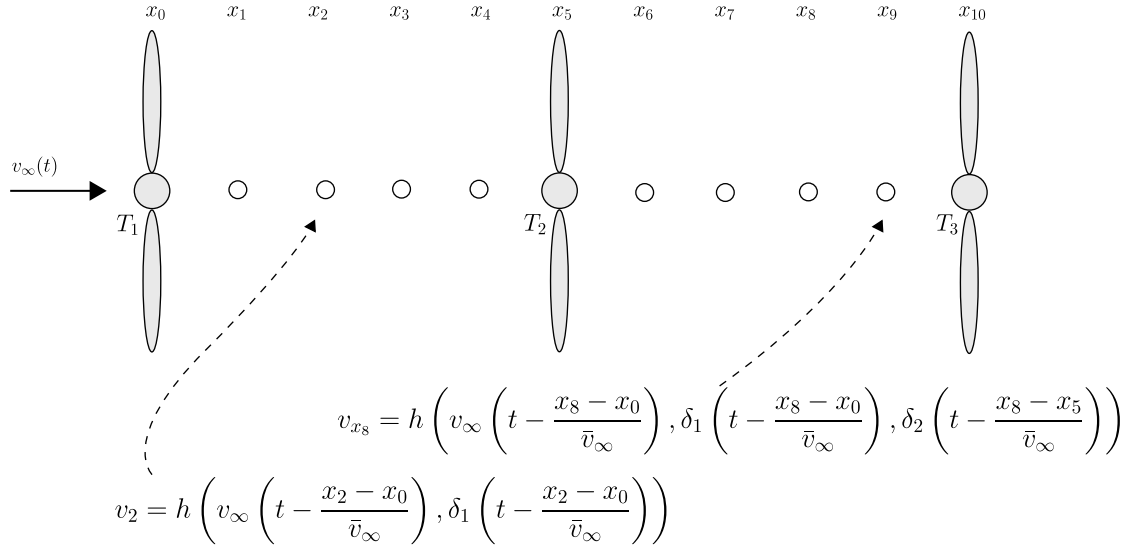


Figure 3: Schematic of Dyanmic Fuga. Propagation of the control variable δ and ambient wake-free wind speed v_∞ is taken into account in the wind flow predictions.

The state-space formulation of the dynamic Fuga model can be expressed as follows:

$$\begin{bmatrix} \underline{\delta}(t + \Delta t) \\ \underline{v}_\infty(t + \Delta t) \end{bmatrix} = \begin{bmatrix} D_l & 0 \\ 0 & D_l \end{bmatrix} \begin{bmatrix} \underline{\delta}(t) \\ \underline{v}_\infty(t) \end{bmatrix} + \begin{bmatrix} E \\ E \end{bmatrix} \begin{bmatrix} \delta(t) \\ v_\infty(t) \end{bmatrix}, \quad (10a)$$

$$\begin{bmatrix} v_{x_1}(t) \\ v_{x_2}(t) \\ \vdots \\ v_{x_n}(t) \\ v_{x_{n+1}}(t) \\ \vdots \end{bmatrix} = \begin{bmatrix} h\left(v_\infty\left(t - \frac{x_1 - x_0}{\bar{v}_\infty}\right), \delta_1\left(t - \frac{x_1 - x_0}{\bar{v}_\infty}\right)\right) \\ h\left(v_\infty\left(t - \frac{x_2 - x_0}{\bar{v}_\infty}\right), \delta_1\left(t - \frac{x_2 - x_0}{\bar{v}_\infty}\right)\right) \\ \vdots \\ h\left(v_\infty\left(t - \frac{x_n - x_0}{\bar{v}_\infty}\right), \delta_1\left(t - \frac{x_n - x_0}{\bar{v}_\infty}\right)\right) \\ h\left(v_\infty\left(t - \frac{x_{n+1} - x_0}{\bar{v}_\infty}\right), \delta_1\left(t - \frac{x_{n+1} - x_0}{\bar{v}_\infty}\right), \delta_2\left(t - \frac{x_{n+1} - x_n}{\bar{v}_\infty}\right)\right) \\ \vdots \end{bmatrix} \quad (10b)$$

where x_0, x_n denote the location of the front turbine and the first downstream turbine in a wind farm. The shaft matrix $D_l \in \mathbb{R}^{N_T N_p \times N_T N_p}$ and $E \in \mathbb{R}^{N_T N_p \times N_T}$ are defined as follows.

$$D_l = \begin{bmatrix} 0 & 0 & \cdots & 0 & 0 \\ I & 0 & \cdots & 0 & 0 \\ 0 & I & \cdots & 0 & 0 \\ \vdots & \vdots & \ddots & \vdots & \vdots \\ 0 & 0 & \cdots & I & 0 \end{bmatrix}, \quad E = [I \ 0 \ 0 \ \cdots]^T \quad (11)$$

Alternatively, the state-space model (10) can be expressed as follows:

$$x_{f,k+1} = A_f x_{f,k} + B_f u_{f,k}, \quad (12a)$$

$$v_k = h_f(x_{f,k}). \quad (12b)$$

To illustrate the effectiveness of the model, Figure 4 shows a steady wind flow of 10 m/s passing through a wind farm with three turbines. All three turbines are following a square-wave derating signal and down-regulating periodically out of phase as shown in Figure 5. Initially in Figure 4a, the first two turbines are operating at full power, creating a significant velocity deficit downstream, whereas the last turbine (turbine 3) turns off and no wake is generated. In Figure 4b, the wake generated by turbine 1 and 2 is propagated downstream. In particular,

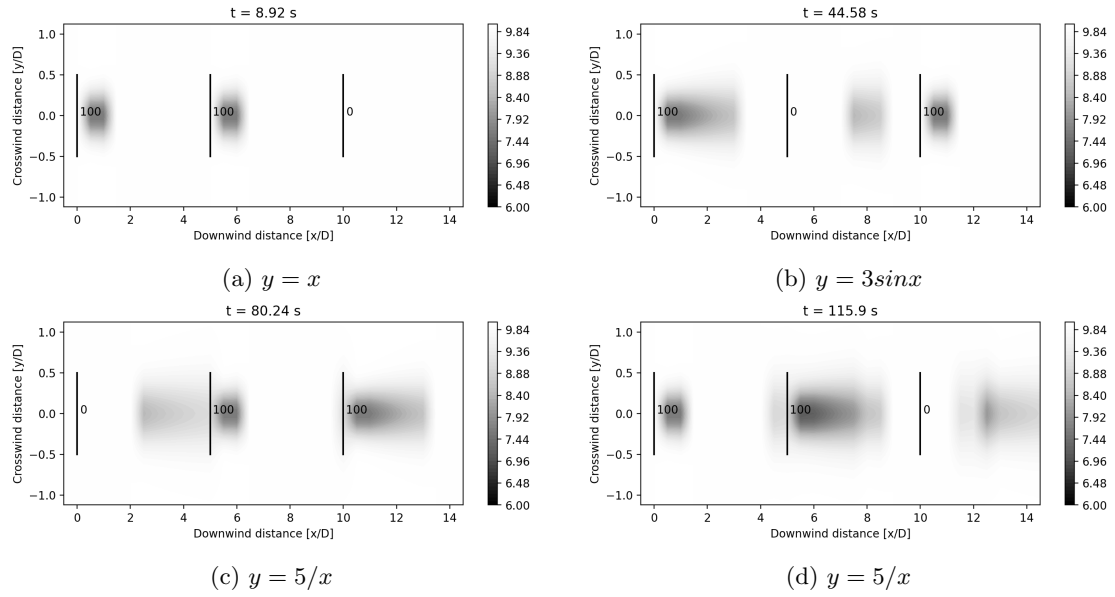


Figure 4: Demonstration of dynamic Fuga. The wake taking into account the control variable and ambient wind speed is propagating downstream at each time step.

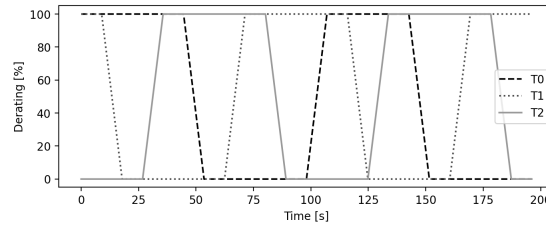


Figure 5: The control signal used in the demonstration of dynamic Fuga.

turbine 2 was off for a period and the wake is still moving toward turbine 3, which cannot be realised solely by the static Fuga alone. In Figure 4c, the wake generated by turbine 1 passed through turbine 2 and in Figure 4d, it can be seen that the wake generated by turbine 1 is superimposed on the wake generated by turbine 2.

1.3 Model predictive controller

This section presents a linear parameter-varying representation of the model that is used in the MPC and then followed by a nonlinear MPC formulation.

1.3.1 Linear parameter-varying representation of the control-oriented models

The turbine and dynamic Fuga model can be represented in a linear parameter-varying (LPV) form as follows:

$$x_{k+1} = Ax_k + B(v_k)u_k \quad (13)$$

$$y_k = Cx_k \quad (14)$$

where $x := [P_1, P_2, \dots]^T \in \mathbb{R}^{N_T}$ is the state vector containing the power output of each turbine (1). The input vector $u \in \mathbb{R}^{N_T}$ contains the power coefficient C_p of each turbine and y_k is the output, which is the total power output of the wind farm. Assuming a slow sample period

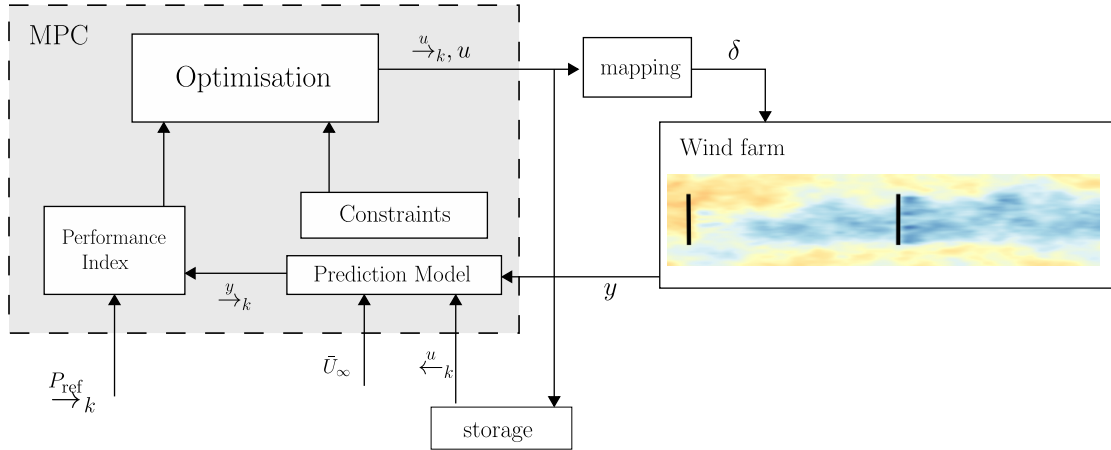


Figure 6: Schematic of the MPC for active power control problems.

(e.g. 5s), the dynamics of the power output can be assumed to be constant. The system matrices $A \in \mathbb{R}^{N_T \times N_T}$, $B \in \mathbb{R}^{N_T \times N_T}$, $C \in \mathbb{R}^{1 \times N_T}$ are defined as follows:

$$A = \begin{bmatrix} 0 & \dots & 0 \\ \vdots & \ddots & \vdots \\ 0 & \dots & 0 \end{bmatrix}, \quad B(v_k) = \begin{bmatrix} \frac{1}{2}\rho\pi r^2 v_1^3 \eta & \dots & \dots & 0 \\ 0 & \frac{1}{2}\rho\pi r^2 v_2^3 \eta & \dots & 0 \\ \vdots & \vdots & \vdots & \vdots \end{bmatrix}, \quad C = [1 \quad 1 \quad \dots] \quad (15)$$

The parameter (wind speed at each turbine) v_j can be predicted using the dynamic Fuga model (12). For the dynamic Fuga model, the input (Power coefficients) of (13) needs to be mapped into derating signals for the dynamic Fuga model.

$$\delta_j = \frac{1}{2}\rho\pi r^2 v_j^3 C_{p,j} \eta / P_{\text{rated}} \quad (16)$$

1.3.2 Formulation of model predictive control

Figure 6 depicts the MPC design for active power control problems. The control task of the MPC is to track the power reference $P_{\text{ref},k}$ or a sequence of future power reference $P_{\text{ref},k}$ if the reference is available in advance. Also, fatigue load reduction also can be part of the control task. MPC computes the future input sequence u_k by solving an optimization problem that takes into account the model prediction, performance index, and constraints. The first input u from the input sequence is applied to the turbine after converting into turbine power set-points via a mapping. The prediction model consists of turbine dynamics and flow dynamics and it takes into account the measurements y from turbines in the wind farm. The measurements can be electrical power and/or tower-base moment if fatigue load reduction is considered in the control objective. In the flow model, the wind speeds at downstream turbines are influenced by the earlier control actions of the upstream. Thus, a storage is employed to store the previous control variables.

Considering a wind farm with the number of turbines denoted by $N_T \in \mathbb{Z}$, an MPC for active

power control problem can be formulated as follows:

$$\min_{\substack{u \\ \rightarrow k}} \sum_{i=0}^{n_c} e_{i|k}^T e_{i|k} \quad (17a)$$

$$\text{s.t. } e_{i|k} = P_{\text{ref},k} - \sum_{j=0}^{N_T} P_{j,i|k}, \quad (17b)$$

$$P_{j,i|k} = \frac{1}{2} \rho A u_{j,i|k} v_{j,i|k}^3 \eta, \quad j = \{1, \dots, N_T\}, \quad (17c)$$

$$v_{j,i|k} = f(u_{\leftarrow k}, u_{\rightarrow k}, \bar{U}_{\leftarrow k}, \bar{U}_{\rightarrow k}), \quad (17d)$$

$$P_{j,0|k} = P_k, \quad (17e)$$

$$P_{j,i|k} \leq P_{\text{rated}}, \quad u_{j,i|k} \leq C_{p,\text{max}}, \quad \Delta P_{j,i|k} \leq \Delta P_{\text{max}}, \quad \forall i, j. \quad (17f)$$

where $k \in \mathbb{Z}$ is the current time step and $j \in \mathbb{Z}$ denotes the index of the turbine. The notation $i|k$ denotes i steps ahead prediction from the current time k . Eq (17a) and (17b) express the control task to minimise the error e between the power reference P_{ref} and electrical power prediction P . The control variable u is the power coefficient C_p . In Eq (17c), ρ, A, η denote the air density, rotor swept area and conversion efficiency. The wind speeds at turbines v are a function of the past and future control variables $(u_{\leftarrow k}, u_{\rightarrow k})$ and average ambient wind speed $\bar{U}_{\leftarrow k}, \bar{U}_{\rightarrow k}$. This wind speed prediction is computed from the proposed dynamic Fuga model, as discussed in the previous section. In Eq (17e), the model is corrected by taking into account the power measurements P_k at current time k . Eq (17f) describes the maximum power output is at the rated power P_{max} and the power coefficient cannot exceed its maximum value C_p . The rate of change in the power ΔP is also limited by its maximum rate ΔP_{max} .

The optimization problem (17) can be represented in terms of the LPV model (13) as follows:

$$\min_{\substack{u \\ \rightarrow k}} \sum_{i=0}^{n_c} (r_{i|k} - y_{i|k})^T (r_{i|k} - y_{i|k}) + u_{i|k}^T \lambda u_{i|k} \quad (18a)$$

$$\text{s.t. } x_{k+1} = Ax_k + B(v_k)u_k, \quad (18b)$$

$$y_k = Cx_k, \quad (18c)$$

$$x_{f,k+1} = A_f x_{f,k} + B_f u_{f,k}, \quad (18d)$$

$$v_k = h_f(x_{f,k}), \quad (18e)$$

$$\underline{u} \leq u_k \leq \bar{u}, \quad \underline{x} \leq x_k \leq \bar{x}, \quad \forall i \quad (18f)$$

Notice that the optimization problem (18) contains an LPV models, thus this cannot be solved directly by standard quadratic programming (QP). One approach is to solve the problem by using gradient-based methods (e.g. [26]), which can be computationally unattractive. Alternatively, quasi-linear MPC can be used [37]. For this problem, the future state sequence x is dependent not only on the future control input u but also on the future scheduling parameter v_k . The parameter variable v is determined by the input u . One can solve the problem (18) by using an iterative approach. By fixing the scheduling parameter trajectory $v_{\rightarrow k}$, the optimization problem (18) can be solved using standard QP solver. Once the input u is found, the parameter trajectory can then be updated and so is the state prediction. Sequentially, the updated QP problem is solved repeatedly until the convergence criteria $|x_k^l - x_k^{l-1}|$ is met.

Furthermore, an additional cost is introduced to penalise the input u . The effect of tuning $\lambda \in \mathbb{R}^{N_T \times N_T}$ can restrict the changes in the control variable, in other words, the change in power set-point. Furthermore, by penalising u , we can demand a higher contribution from the downstream turbine and achieve load equalisation objective.

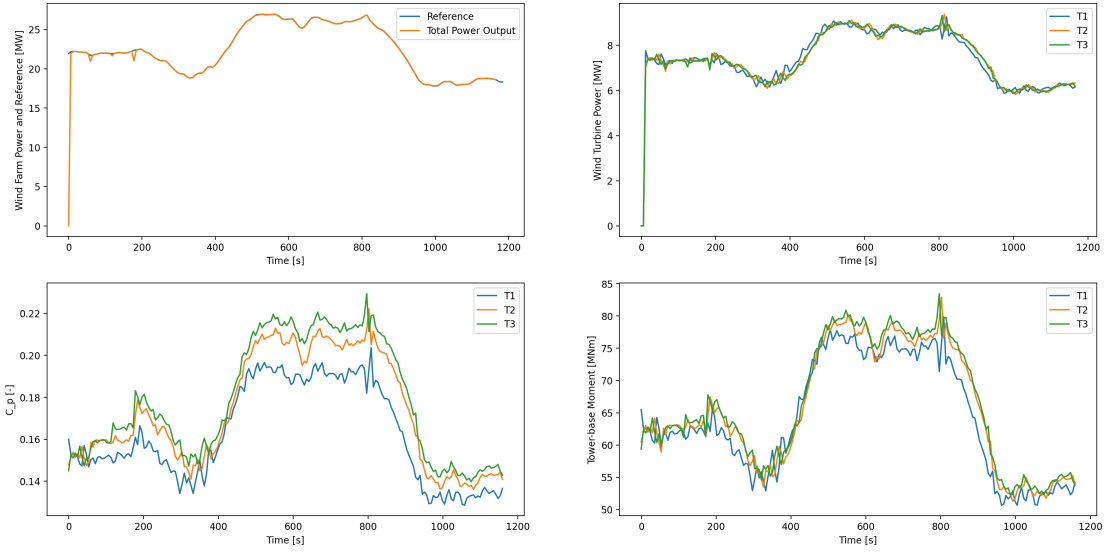


Figure 7: High wind speed case $\bar{U} = 15$ m/s. Top-left: reference signal from the TSO and wind farm power output. Top-right: individual turbine power outputs. Bottom-left: power coefficient (control variable) of each turbine. Bottom-right: Tower-base fore-aft bending moments of each turbine.

1.4 Numerical simulations

This section will demonstrate the effectiveness of the proposed MPC and its capability to track the power reference from the TSO. Also, it will be shown how the MPC can handle load equalisation objective while performing active power control.

1.4.1 Simulation set-up

The wind farm used in this study is a three turbines in a row example, as illustrated in Figure 3. Three turbines are 5 rotor-diameters away from each other in the stream-wise direction. The turbines used in this study is the DTU 10-MW reference wind turbine [38]. To demonstrate the concept, the simulation platform used is also the Dynamic Fuga model. Future work will use a higher fidelity wind farm simulator such as HAWC2Farm.

The wind farm reference signal used in this study is developed based on the regulation signal "RegD", obtained from PJM, an independent system operator in the eastern United States [21]. The wind farm reference signal is defined as follows:

$$\bar{P} = \min\left(\frac{1}{2}\rho A \bar{U}^3 C_{p,\max} N_T, P_{\text{rated}} N_T\right), \quad (19)$$

$$P_{\text{ref}} = 0.7\bar{P} + 0.2\bar{P}r_D, \quad (20)$$

where r_D denotes the RegD signal whilst \bar{P}, \bar{U} denote the time-averaged power generated by the wind farm under 'greedy strategy' and time-averaged wind speed in the past, respectively.

1.4.2 High wind speed case

The flow field at hub-height in front of the farm has a mean wind speed of 15 m/s in the stream-wise direction and turbulence intensity of 5%. The simulation sample time is chosen to be 6 s. This wind speed is sufficiently high for all turbines in the wind farm to generate the rated power.

The performance of the MPC is shown in Figure 7. The tracking performance of the MPC was remarkable, where the reference from the TSO is closely matched with the power generated by

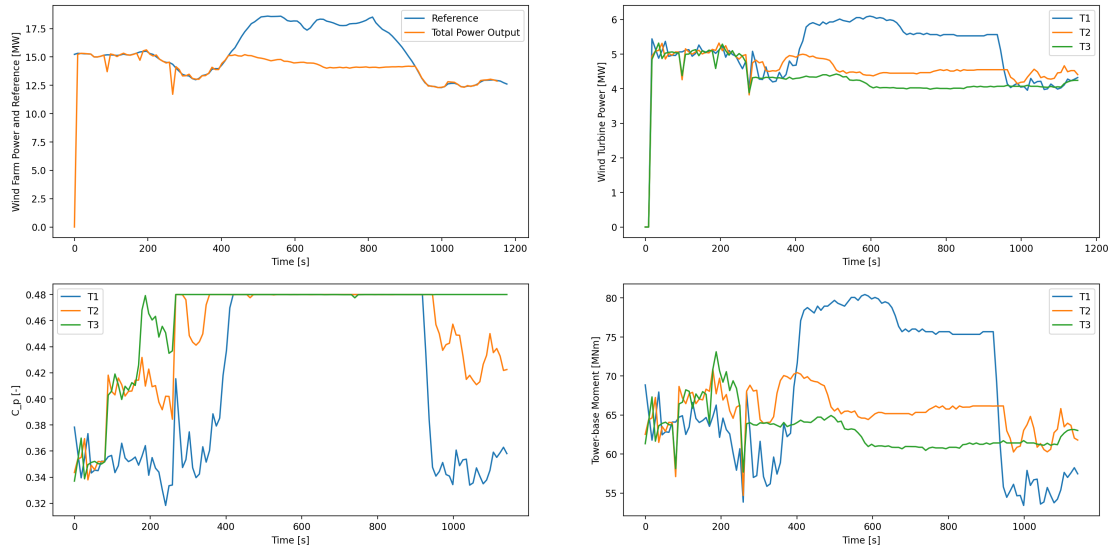


Figure 8: Low wind speed case $\bar{U} = 10$ m/s. Top-left: reference signal from the TSO and wind farm power output. Top-right: individual turbine power outputs. Bottom-left: power coefficient (control variable) of each turbine. Bottom-right: Tower-base fore-aft bending moments of each turbine.

the wind farm. Furthermore, by formulating the cost function to penalise the upstream turbine control variable (C_p), the power output is distributed fairly and tower-base fore-aft loads between turbines are shared equally.

However, there are some limitations of the wind farm simulator on the load aspect. Since the turbine tower load is computed based on the aerodynamic thrust multiplied by the turbine hub-height and the sampling period is relatively large, the true turbulent effect on the loads might not be able to be revealed by the farm simulator.

1.4.3 Low wind speed case

This section presents a case where the wind speed is not sufficient to produce the requested power from the TSO. The wind speed at hub-height in front of the farm has a mean wind speed of 10 m/s in the stream-wise direction and turbulence intensity of 5%. The simulation sample period is 9 s.

Figure 8 shows the performance of the proposed MPC in a low wind speed case. It can be seen that between 400s and 900s, the available power is not sufficient to generate the requested power from the TSO. The MPC minimised the tracking error by operating downstream turbines at a higher output, which gives the highest available power in the wind farm. Notice that the result might be counter-intuitive. This is because the result is highly dependent on the wind farm simulator. That means that it is not necessary that the downstream turbines operating at the highest power would result in the highest power output of the wind farm. It could be that the wake velocity deficit in the Fuga model is less severe compared to other models.

1.5 Conclusions

The study presents a model predictive control design for wind farm active power control problem. In particular, a dynamic flow model (Dynamic Fuga) is developed for the MPC in this study, where the model is formulated based on a static flow model (Fuga) and incorporation of the time propagation of the control variables and the ambient wake-free wind speeds. Two investigations were performed in the numerical simulations: (i) high wind speed case and (ii) low wind speed

case. The proposed MPC controller managed to track the power requested by the TSO in a high wind speed situation. In the case of low wind speed, the MPC minimises the error between the reference and wind farm power output. Future work will validate the proposed method on a higher fidelity wind farm simulator such as HAWC2Farm. In addition, the proposed method will also be tested on a larger wind farm such as the TotalControl Reference Wind Power Plant.

2 CLOSED LOOP CONTROL BASED ON GAUSSIAN WAKE MODEL

2.1 Introduction

Large wind farms suffer from performance losses due to the wake interactions between different turbine rows within the farm. The prevailing control paradigm in industry does not account for these interactions and instead optimizes operations at the individual turbine level. Consequently, currently operational wind farms operate at a reduced power extraction efficiency with unnecessarily high fatigue loading. In recent years, the prospect of mitigating harmful wake interactions in a wind farm through the use of coordinated wind-farm control has inspired many research efforts. Amongst wind farm control strategies, wake-steering has emerged as a popular technique by which wakes of upstream turbines in a farm are redirected from the downstream turbines through yaw control. Axial induction control is another coordinated control methodology, in which wind turbines are made to operate at non-ideal operating set-points, which leads to weaker wakes and hence higher power extraction by downstream turbines.

A previous TotalControl deliverable used an offline wake model to determine optimal wake steering set-points for two wind farms operating under different atmospheric conditions, with the goal of maximising overall wind farm power production [39]. These set-points were thereafter tested through simulations in a high fidelity LES environment (without feedback), to validate an open-loop control methodology. While significant power gains were obtained, further analysis exhibited discrepancies in the predictions from the wake model and the measurements from LES. These errors arise due to an inherent weakness of the wake models, whose accuracy depends upon analytical wake expansion parameters which may not be reliable for all operating conditions. Additionally, in the previous open-loop control simulations, it was assumed that the atmospheric conditions remain unchanged, something which is not realistic for wind farms in the field that are constantly subjected to varying inflow conditions. To overcome these shortcomings, a closed-loop control methodology is developed in which measurements are taken from the LES domain for calibrating the wake model parameters for improved predictions. A closed-loop framework with feedback would also allow for dynamically changing inflow conditions which is essential to accurately control wind farms to obtain the desired objective.

This part is organised as follows: First, a reference wind farm database is detailed which is used as a basis to showcase the effect of closed-loop control. Then, the different aspects of the closed-loop control framework are detailed. The next section details the results in which comparisons are made between open-loop and closed-loop control on the basis of power production, yaw dynamics and fatigue accumulation in the turbines. Finally, the conclusions and future work are outlined in the last section.

2.2 Reference database

The wind farm considered in this study is the TotalControl Reference Wind Power Plant (TC-RWP), which is a virtual wind farm designed to develop coordinated wind-farm control strategies, and has been previously used to develop a publicly available reference wind-farm database comprising of LES numerical measurements spanning different atmospheric conditions and wind directions across the farm. The farm consists of 32 DTU 10 MW turbines [40], separated by 5D stream-wise and span-wise spacing in a 4 row configuration, as seen in Figure 9. The database is composed of power, velocity and blade loading time series from all the turbines, across different inflow conditions and wind directions. Two different boundary layers types, Pressure Driven Boundary Layers (PDBL) and Conventionally Neutral Boundary Layers (CNBL), are fed into the wind farm using the precursor method and the operation is simulated in SP-Wind, an in-house aeroelastic LES code developed at KU Leuven over the past 15 years [41, 42, 43]. Specifications of the different cases from the reference database used in this study are detailed

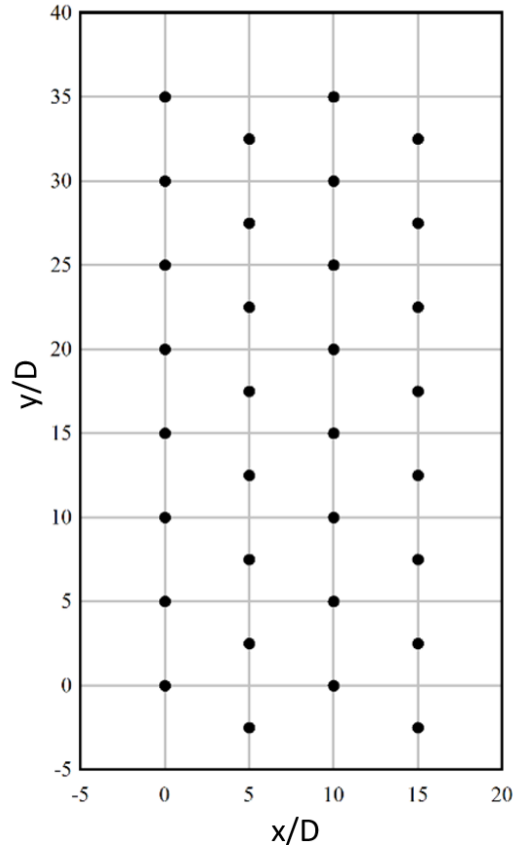


Figure 9: Planview of TCRWP layout comprising of 32 DTU 10 MW turbines. Turbines are numbered 1 to 32 bottom to top and left to right.

in Table 1, where Pdk refers to the PDBL inflows and CNk refers to the CNBL inflows. The subscripts 2 and 4 for the CNBL cases denote the capping inversion strength, and all the inflows have a base wall roughness length of $z_0=2 \times 10^{-4}$ m. Additional information about the database can be found in the publicly available zenodo repositories [44, 45, 46, 47, 48, 49].

2.3 Closed loop control

An overview of the closed-loop methodology is shown in Figure 10, and the following subsections elaborate on its different components.

Table 1: Specifications of the reference database

Case No.	Inflow	Wind direction	Hub height wind speed	Hub height TI
1	Pdk	0°	9.4 m s^{-1}	5.15%
2	CNk_2	300°	11.0 m s^{-1}	3.66%
3	CNk_2	330°	11.0 m s^{-1}	3.66%
4	CNk_4	300°	11.3 m s^{-1}	3.65%
5	CNk_4	0°	11.3 m s^{-1}	3.65%

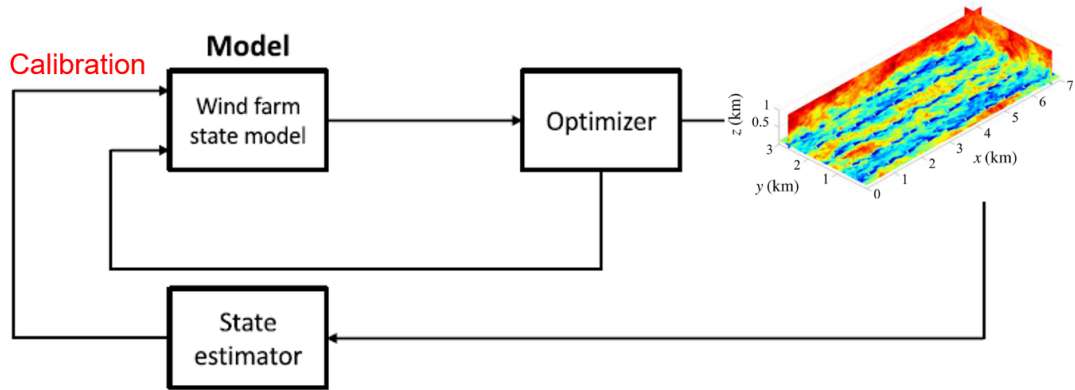


Figure 10: Closed loop wind farm control methodology. Calibration is required based on measurements from a plant to improve state model. LES is used as a substitute for real wind farm operation.

Table 2: Summary of the general domain and time parameters for LES in SP-Wind

Domain size	$L_x \times L_y \times L_z$	$16 \times 16 \times 1.5$ km
Grid	$N_x \times N_y \times N_z$	$1200 \times 1200 \times 225$
Resolution	$\Delta_x \times \Delta_y \times \Delta_z$	$13.33 \times 13.33 \times 6.66$ m
Wind farm spin-up time	T_{spin}	15 min
Simulation time	T	60 min
LES time step	Δt_{LES}	0.5 s
Structural time step	Δt_{MBS}	0.01 s

2.3.1 Flow model - SP-Wind

The Flow model used to test the optimally determined set-points is SP-Wind, an in-house Large Eddy Simulation code built on a high-order flow solver developed over the last 15 years at KU Leuven [50, 51, 52]. SP-Wind solves the three-dimensional, unsteady, and spatially filtered Navier-Stokes momentum and temperature equations, with wind turbines contributing to the forcing terms in the equations. Spatial discretization is performed in the horizontal and span-wise directions by using pseudo-spectral schemes while a vertical fourth-order energy-conservative finite differences are used in the vertical direction. The equations are marched in time using a fully explicit fourth-order Runge-Kutta scheme, and grid partitioning is achieved through a scalable pencil decomposition approach. The turbines in the flow domain are parameterized using the Aeroelastic Actuator Sector Method (AASM) [53]. Subgrid-scale stresses are modeled with a standard Smagorinsky model with Mason and Thomson wall damping [51].

Wind farm simulations are run for a period of 75 minutes, which includes a 15 minute start-up period for the settling of initial transients. The entire wind farm is rotated in the flow domain to simulate different wind directions. The structural and aerodynamic properties of the DTU 10 MW turbine tower and blades, and the DTU Wind energy controller are used to simulate the turbine operation [40]. Numerical specifications of the LES are provided in Table 2.

2.3.2 State estimation

In order to optimize the performance of the wind farm, the state model, which is detailed in the next section, requires information regarding the current operating conditions of the turbines within the farm. This includes the following:

- Power production of all turbines
- Current control states of all turbines (yaw angle, pitch angle, rotational speed)
- Inflow wind speed
- Inflow turbulent intensity
- Wind direction.

While the first 2 items are readily available as measurements or outputs of the wind farm, accurate measurements of the latter 3 items are not usually available in commercial wind farms and need to be estimated. In the current work, we focus on estimating the inflow wind speed of the farm, while the turbulence intensity and wind direction are taken directly from the reference database detailed in Table 1.

The inflow wind speed is estimated by the following expression,

$$U_b = \underset{\tilde{U}_b}{\operatorname{argmin}} \left(\frac{1}{N_U} \sum \left(\bar{P}_i - \hat{P}_i(\phi, \tilde{U}_b, \tilde{\gamma}_i) \right)^2 \right) \quad (21)$$

where \bar{P}_i is the time averaged power output from LES and \hat{P}_i is the predicted power by the wind farm state model, per turbine i . N_U is a set of the upstream wind turbines of the farm, which has been previously determined based on the wind direction ϕ . The averaging time for the measurements depends upon the sampling time t_s , which is the regular constant time interval after which the closed-loop control framework is executed.

2.3.3 Wake model

In the developed closed-loop control, an analytical wake model serves as the state model for the wind farm operation which is used for optimizing performance. Assuming that the wakes in the wind farm are carried by the background flow $\mathbf{U}_b(\mathbf{x})$, the flow field in the farm is then given by the velocity field \mathbf{U}_{N_t} , which is constructed using the recursive formula [54]

$$\mathbf{U}_i(\mathbf{x}) = (\mathbf{U}_{i-1}(\mathbf{x}) \cdot \mathbf{e}_{\perp,i}) \mathbf{e}_{\perp,i} (1 - W_i(\mathbf{x})) + (\mathbf{U}_{i-1}(\mathbf{x}) \cdot \mathbf{e}_{\parallel,i}) \mathbf{e}_{\parallel,i}, \quad \text{for } i = 1, \dots, N_t \quad (22)$$

The starting term of the recursion is given by $\mathbf{U}_o(\mathbf{x}) = \mathbf{U}_b(\mathbf{x})$, which is an input to the model. Unit vectors $\mathbf{e}_{\perp,i} = (\cos\theta_i, \sin\theta_i)$ and $\mathbf{e}_{\parallel,i} = (-\sin\theta_i, \cos\theta_i)$ account for the incoming wind direction and yaw angle at turbine i . The wake deficit W_i is evaluated using the Bastankhah model [55], according to which the wake deficit behind a yawed turbine is evaluated as a function of stream-wise coordinates using the equation

$$W(\mathbf{x}) = \left(1 - \sqrt{1 - \frac{C_T \cos\gamma}{8\sigma_x \sigma_y}} \right) \exp \left[-\frac{1}{2} \left\{ \left(\frac{z - z_h}{\sigma_z} \right)^2 + \left(\frac{y - \delta}{\sigma_y} \right)^2 \right\} \right] \quad (23)$$

where γ is the turbines yaw angle, C_T is the wind turbine thrust set-point coefficient, δ is the wake deflection and D is the turbine rotor diameter. σ_y and σ_z are wake widths of the turbine at the downstream location, which in turn depend upon the wake growth rate k_w and the near-wake length x_0 according to the following expressions

$$\frac{\sigma_y}{D} = 0.35 \cos\gamma + k_w \ln \left[1 + \exp \left(\frac{x - x_0}{D} \right) \right] \quad (24)$$

$$\frac{\sigma_z}{D} = 0.35 + k_w \ln \left[1 + \exp \left(\frac{x - x_0}{D} \right) \right] \quad (25)$$

Further details of the wake deficit model and its parameters can be found in the references [55, 56]. The inflow velocity of each turbine i is finally evaluated across the disc area at observation

points which are distributed across the disc according quadrature rule with $N_q = 16$ points. The quadrature-point coordinates are denoted by $x_{k,q}$ and are chosen following the rule proposed by Holoborodko with uniform weighting factor of $w_q = 1/N_q$ [57]. The inflow velocity at each turbine, S_i , is therefore calculated as

$$S_i = \sum_{q=1}^{N_q} w_q S(x_{i,q}) \quad (26)$$

Where, $S(x) = \|U(x)\|_2$. The inflow velocity at each turbine is then finally used to evaluate the power production of the turbine, which is obtained by interpolating the performance curve of the DTU 10 MW turbine [40].

2.3.4 Model tuning

The analytical model referred to section 2.3.1 is used to evaluate the performance of the TCRWP, simulating the same cases as the reference wind-farm database [58]. Wake expansion parameters k_{w_i} of every turbine in the farm are then optimally tuned to minimize the error between individual wind turbine power production as predicted by the wake model and SP-Wind. The minimization problem for parameter tuning can thus be defined as

$$\min_{\omega} \frac{1}{N_t} \sum_{i=1}^{N_t} \left(\bar{P}_i - \hat{P}_i(\omega) \right)^2 + \lambda \sum_{i=1}^{N_t} \omega_i^2 \quad (27)$$

where $\omega = k_{w_1}, k_{w_2}, \dots, k_{w_{N_t}}$ is a vector comprising of wake expansion parameters of the turbines within a farm. To prevent over-fitting of the model, a regularizing penalty term is introduced in the above optimization problem using ridge-regression through the ridge parameter λ [59]. The minimization problem is subsequently solved using the SLSQP solver from the SciPy package [60].

2.3.5 Optimization methodology

Having computed the inflow velocities at each turbine through the wake model, and after tuning the model based on the current power measurements within the farm, an optimization problem can be defined to maximise the total wind farm power prediction as follows

$$\begin{aligned} \min_{\gamma} \quad & -1 * \sum_{k=1}^{N_t} \frac{1}{2} \rho C_P(\gamma_k) A_k U_k^3(\gamma), \\ \text{s.t.} \quad & -\frac{\pi}{6} < \gamma < \frac{\pi}{6}. \end{aligned} \quad (28)$$

In the above equation, C_P is the coefficient of power of each turbine, evaluated for a yaw angle γ_k according to the cosine power law [61]. γ is a vector containing the yaw set-points for all the turbines across the farm, $\gamma = [\gamma_1, \gamma_2, \dots, \gamma_{N_t}]$. The optimization problem is then solved to obtain optimal yaw angles for all the turbines within the wind farm using the SLSQP solver from the SciPy Python package, while utilizing the multi-start approach of basin-hopping to avoid local minima [60]. The optimization methodology has been previously used for determining optimal wake steering set-points for the TCRWP for the reference database though wake steering, exhibiting gains up to 25% [62]. The methodology has also been extended to include the effect of induction control by changing the thrust set-points of the turbine through pitch or rotational speed control [63].

2.3.6 Formulation of closed-loop control

The formulation of the closed-loop control framework is summarized in Figure 11. Since the developed wake model makes use of a static wake model, model dynamics are accounted for in a

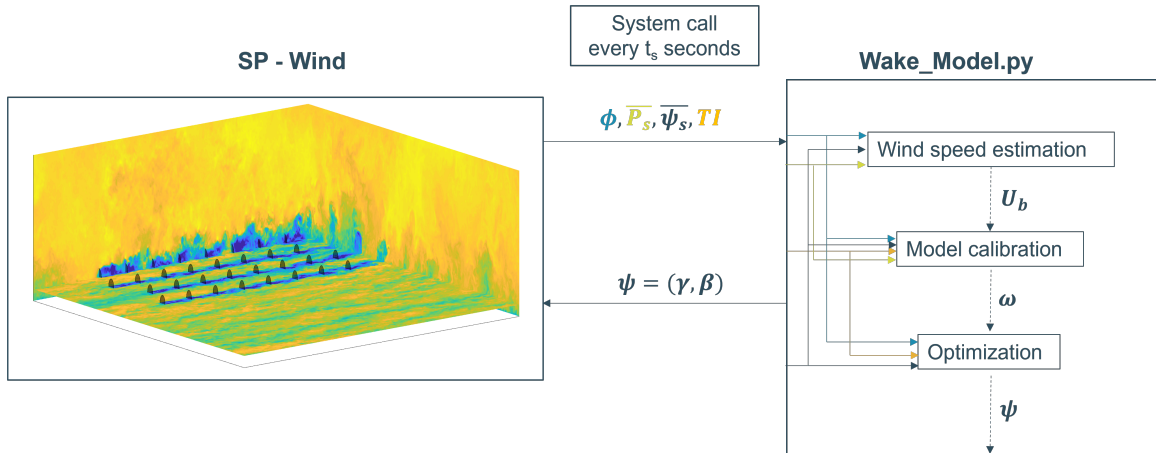


Figure 11: Flow of information in the quasi-static closed-loop control framework.

quasi-static sense by executing the closed-loop framework at regular fixed intervals of t_s . At each optimization step, the Fortran based LES code SP-Wind calls the python based analytical wake model through system calls. Time averaged measurements are then taken from the wind farm operating in the LES domain, which are then used to first estimate the inflow wind speed, followed by model calibration and finally wind farm performance optimization. The turbine control parameters are designated by Ψ , and include the optimal yaw set-point for all the turbines within the farm to obtain the optimization objective. While induction control and fatigue minimization can be included in the objective function, the current work is limited to power maximization through wake steering for simplicity. The choice of sampling time t_s can have a major impact on the performance of the framework and the resulting wind farm performance, but as a first step it is set to 10s. Once the optimal set-points are determined, they are sent back to SP-Wind. The turbines in the LES domain track the dynamically changing set-points based on the yaw and pitch rate limitations of their actuators, which are 0.3 deg/s and 10 deg/s respectively for the DTU10 MW turbine.

2.4 Results

2.4.1 Wind farm power production

Total wind farm power gains obtained via closed-loop control, and a comparison against the gains obtained from open-loop control is shown in Figure 12. In both the control methodologies, the base case is taken as when all the turbines are operating in 'greedy' control. While significant power gains are obtained through wake steering in all the cases, closed-loop control appears to outperform open-loop control in only two out of the five cases from Table 1. This could be attributed to two factors. Firstly, in a previous work it was observed that the deepest 8 turbine arrays of cases 1 and 5 due to a northerly wind direction lead to higher errors when comparing the power predicted by the wake model and LES [64]. Therefore, the calibration step in the developed closed-loop framework leads to improvement of the state model, resulting in optimal wind farm yaw set points which produce higher farm-wide power production for only these two cases. Secondly, the chosen sampling time of t_s in the current study could have been too short, resulting in a large variation in the estimated inflow conditions, leading to a large variation in the optimal yaw angles determined by the model due to the sensitivities of the wake model, as remarked upon in previous literature [61]. This is evident from Figures 13 and 14, which show the large variability of the yaw angles. Large jumps in yaw angles during the simulation time can be observed, with some turbines changing from a large positive angle to a large negative angle. These large jumps could have a detrimental effect on turbine performance due to unsteady aerodynamics and cause yaw fatigue.

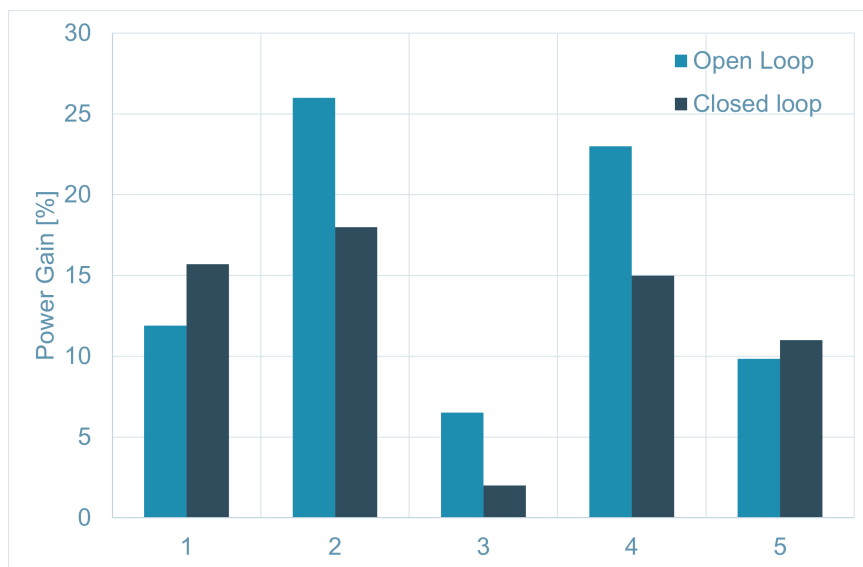


Figure 12: Total wind farm power gains for closed-loop and open-loop control with respect to greedy control.

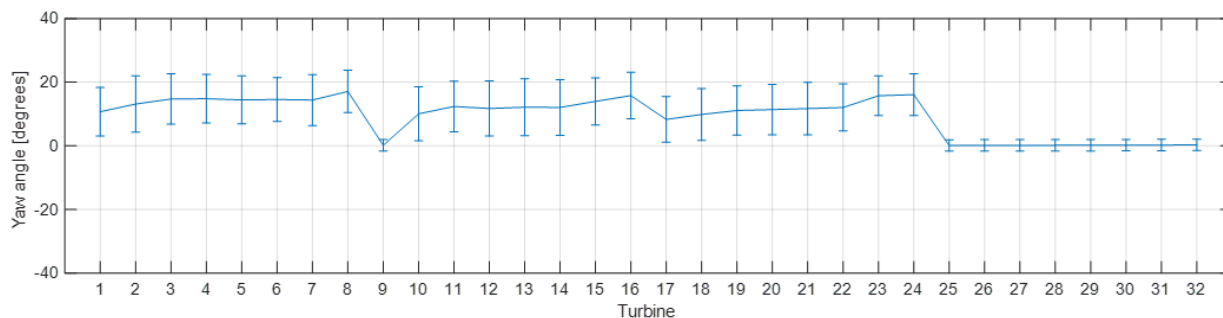


Figure 13: Variability of optimal yaw angles determined by the wake model for case 4.

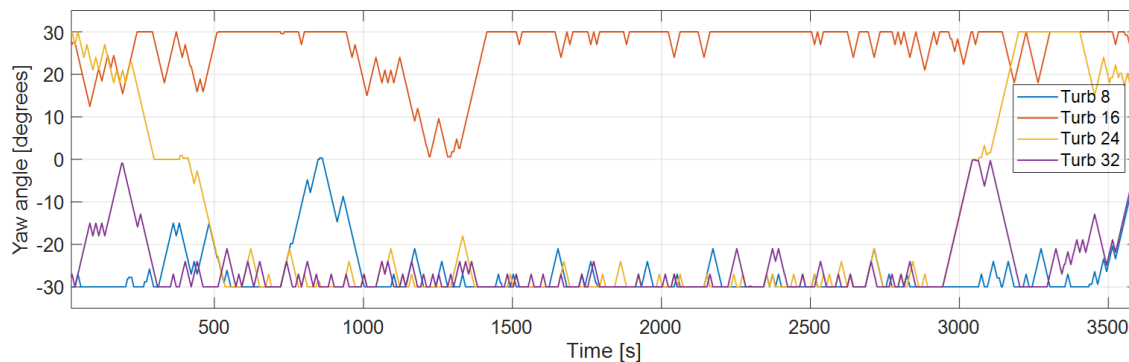


Figure 14: Optimal yaw angles time series for 4 upstream turbines in case 5.

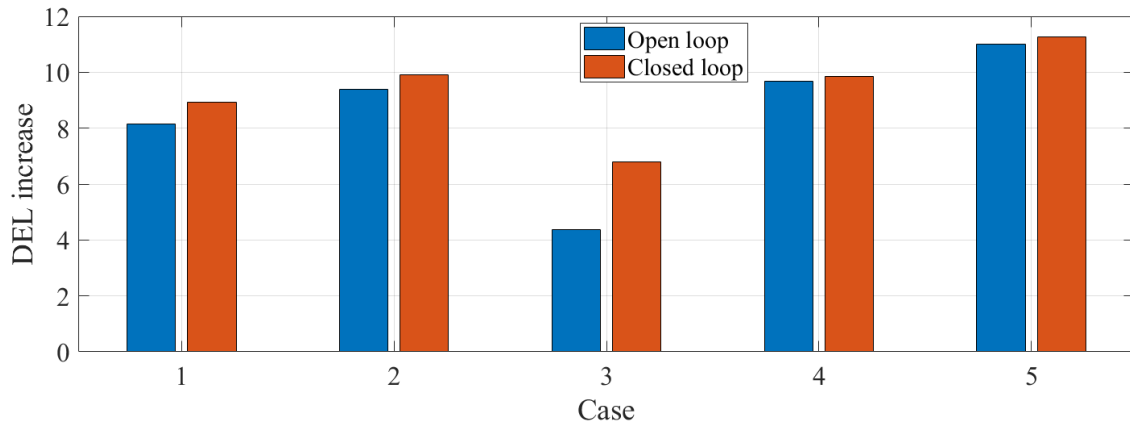


Figure 15: Total wind farm blade root flapwise DEL gains for closed-loop and open-loop control with respect to greedy control.

2.4.2 Effect on fatigue

To determine the effect of closed loop control and the observed excessive yaw variation on the structure of the turbines, we use Damage Equivalent Loads (DELs) to quantify the increase in fatigue when compared against open-loop optimization. DEL of each turbine is computed using the Palmgren–Miner rule and the Wöhler equation to account for accumulating fatigue damage caused to the wind turbine components by the fluctuating structural loads [65]. The loads time series are counted and binned into individual cycles using the rainflow-counting algorithm [66], and for the wind turbine blades the components follow the Wöhler’s curve with a slope coefficient equal to 10. Results of the DEL analysis are presented in Figure 15, in which the cumulative flapwise root bending DEL increase is compared for the open-loop and closed-loop control methodologies against the base greedy reference operation. A direct consequence of the larger yaw variation can be seen in the increase in cumulative DEL in the closed-loop control when compared to open-loop control. This implies increased fatigue accumulation and shortened operational life-time of turbine blades.

2.5 Conclusions and future work

In this work, a closed-loop control framework was developed which used an analytical wake model as the wind farm state model for optimizing power production in LES. Through online state estimation, model calibration and optimal wake steering, the power production of a reference wind farm was increased when compared to a base greedy operation case. When compared to open-loop control, it was observed that in only 2 of the tested 5 cases the closed-loop controller was able to outperform previously obtained open-loop control results. This could be attributed to the large variation in the optimal yaw angles during the operation of the wind farm. The increased variation in yaw angles also lead to increase in turbine fatigue. Future work will focus on improving the closed-loop control framework by investigating the effect of sampling time and addressing the strong yaw angle jumps. The framework could also be extended by incorporating turbulence intensity and wind direction estimators to increase its usability in a real wind farm environment. Furthermore, testing the framework while subjected to dynamically changing inflow conditions could also be of interest.

REFERENCES

- [1] Jacob Aho, Andrew Buckspan, Lucy Pao, and Paul Fleming. An Active Power Control System for Wind Turbines Capable of Primary and Secondary Frequency Control for Supporting Grid Reliability. *AIAA/ASME Wind Symposium*, pages 1–13, 2013.
- [2] S. Boersma, B. M. Doekemeijer, T. Keviczky, and J. W. Van Wingerdenl. Stochastic model predictive control: Uncertainty impact on wind farm power tracking. *Proceedings of the American Control Conference*, 2019-July:4167–4172, 2019.
- [3] Poul Sørensen, Anca D Hansen, Florin Iov, Frede Blaabjerg, Martin H Donovan, Poul Sørensen, Anca D Hansen, Florin Iov, Frede Blaabjerg, and Martin H Donovan. *Wind farm models and control strategies*, volume 1464. 2005.
- [4] Anca D. Hansen, Poul Sørensen, Florin Iov, and Frede Blaabjerg. Centralised power control of wind farm with doubly fed induction generators. *Renewable Energy*, 31(7):935–951, 2006.
- [5] JD Grunnet, M. Soltani, Torben Knudsen, M. Kragelund, and Thomas Bak. Aeolus toolbox for dynamics wind farm model, simulation and control. In *Proc. of EWEC*, 2010.
- [6] Mahmood Mirzaei, Mohsen Soltani, Niels K. Poulsen, and Hans H. Niemann. Model based active power control of a wind turbine. In *2014 American Control Conference*, number July 2016, pages 5037–5042. IEEE, 2014.
- [7] Yunho Jeong, Kathryn Johnson, and Paul Fleming. Comparison and testing of power reserve control strategies for grid-connected wind turbines. *Wind Energy*, 17(3):343–358, 2014.
- [8] Kuichao Ma, Jiangsheng Zhu, Mohsen Soltani, Amin Hajizadeh, and Zhe Chen. Wind turbine down-regulation strategy for minimum wake deficit. *2017 11th Asian Control Conference (ASCC)*, pages 2652–2656, 2017.
- [9] Wai Hou Lio, Mahmood Mirzaei, and Gunner Chr. Larsen. On wind turbine down-regulation control strategies and rotor speed set-point. *Journal of Physics: Conference Series*, 1037:032040, 2018.
- [10] Jan-Willem van Wingerden, Lucy Pao, Jacob Aho, and Paul Fleming. Active Power Control of Waked Wind Farms. *IFAC-PapersOnLine*, 50(1):4484–4491, 2017.
- [11] V. Petrović, J. Schottler, I. Neunaber, M. Hölling, and M. Kühn. Wind tunnel validation of a closed loop active power control for wind farms. *Journal of Physics: Conference Series*, 1037(3), 2018.
- [12] M. Vali, V. Petrović, G. Steinfeld, L. Y. Pao, and M. Kühn. Large-eddy simulation study of wind farm active power control with a coordinated load distribution. *Journal of Physics: Conference Series*, 1037(3), 2018.
- [13] Mehdi Vali, Vlaho Petrović, Gerald Steinfeld, Lucy Y. Pao, and Martin Kühn. An active power control approach for wake-induced load alleviation in a fully developed wind farm boundary layer. *Wind Energy Science*, 4(1):139–161, 2019.
- [14] V Spudic. Hierarchical wind farm control for power/load optimization. *Proc. of The Science of making Torque from Wind*, 2010.
- [15] V. Spudic, M. Jelavic, and M. Baotic. Wind turbine power references in coordinated control of wind farms. *Automatika–Journal for Control, Measurement, Electronics, Computing and Communications*, 52(2):82–94, 2011.
- [16] Daria Madjidian, Karl Martensson, and Anders Rantzer. A Distributed Power Coordination Scheme for Fatigue Load Reduction in Wind Farms. *Proceedings of the 2011 American Control Conference*, pages 5219–5224, 2011.

- [17] V. Spudic, C. Conte, M. Baotic, and M. Morari. Cooperative distributed model predictive control for wind farms. *Optimal Control Applications and Methods*, 2014.
- [18] Haoran Zhao, Qiuwei Wu, Qinglai Guo, Hongbin Sun, and Yusheng Xue. Distributed Model Predictive Control of a Wind Farm for Optimal Active Power Control Part II: Implementation With Clustering-Based Piece-Wise Affine Wind Turbine Model. *IEEE Transactions on Sustainable Energy*, 6(3):840–849, 2015.
- [19] Sjoerd Boersma, Vahab Rostampour, Bart Doekemeijer, Will van Geest, and Jan-Willem van Wingerden. A constrained model predictive wind farm controller providing active power control: an LES study. *Journal of Physics: Conference Series*, 1037:032023, 2018.
- [20] Mehdi Vali, Vlaho Petrovi, Lucy Y Pao, and K Martin. Model Predictive Active Power Control for Optimal Structural Load Equalization in Waked. pages 1–16, 2021.
- [21] C Pilong. PJM Manual 12: Balancing Operations. Technical report, technical report, PJM, 2013.
- [22] Christopher J. Bay, Jennifer Annoni, Timothy Taylor, Lucy Pao, and Kathryn Johnson. Active Power Control for Wind Farms Using Distributed Model Predictive Control and Nearest Neighbor Communication. *Proceedings of the American Control Conference*, 2018-June(August):682–687, 2018.
- [23] P. M.O. Gebraad, F. W. Teeuwisse, J. W. Van Wingerden, P. A. Fleming, S. D. Ruben, J. R. Marden, and L. Y. Pao. A data-driven model for wind plant power optimization by yaw control. *Proceedings of the American Control Conference*, pages 3128–3134, 2014.
- [24] S. Boersma, P.M.O. Gebraad, M. Vali, B.M. Doekemeijer, and J.W. van Wingerden. A control-oriented dynamic wind farm flow model: “WFSim”. In *Journal of Physics: Conference Series*, volume 753, page 032005, 2016.
- [25] Mehdi Vali, Vlaho Petrović, Sjoerd Boersma, Jan-Willem van Wingerden, and Martin Kühn. Adjoint-based model predictive control of wind farms: Beyond the quasi steady-state power maximization. *IFAC-PapersOnLine*, 50(1):4510–4515, 2017.
- [26] Mehdi Vali, Vlaho Petrović, Sjoerd Boersma, Jan Willem van Wingerden, Lucy Y. Pao, and Martin Kühn. Adjoint-based model predictive control for optimal energy extraction in waked wind farms. *Control Engineering Practice*, 84(September 2018):48–62, 2019.
- [27] Jonas Kazda and Nicolaos Antonio Cutululis. Fast control-oriented dynamic linear model of wind farm flow and operation. *Energies*, 11(12), 2018.
- [28] Jonas Kazda and Nicolaos A. Cutululis. Model-optimized dispatch for closed-loop power control of waked wind farms. *IEEE Transactions on Control Systems Technology*, 28(5):2029–2036, 2020.
- [29] Søren Ott and Morten Nielsen. Developments of the offshore wind turbine wake model Fuga. 2014.
- [30] Pieter M.O. Gebraad and J. W. Van Wingerden. A control-oriented dynamic model for wakes in wind plants. *Journal of Physics: Conference Series*, 524(1), 2014.
- [31] Morten Hartvig Hansen and Lars Christian Henriksen. Basic DTU Wind Energy controller. Technical Report January, 2013.
- [32] Christos Galinos, Jonas Kazda, Wai Hou Lio, and Gregor Giebel. T2FL: An efficient model for wind turbine fatigue damage prediction for the two-turbine case. *Energies*, 13(6), 2020.
- [33] Jacob Aho, Andrew Buckspan, and Jason H. Laks. A tutorial of wind turbine control for supporting grid frequency through active power control. *Proc. of the American Control Conference*, pages 3120–3131, 2012.

- [34] Alfredo Penã, Kurt Schaldemose Hansen, Søren Ott, and Maarten Paul Van Der Laan. On wake modeling, wind-farm gradients, and AEP predictions at the Anholt wind farm. *Wind Energy Science*, 3(1):191–202, 2018.
- [35] Maarten Paul van der Laan, Søren Juhl Andersen, Néstor Ramos García, Nikolas Angelou, Georg Raimund Pirrung, Søren Ott, Mikael Sjöholm, Kim Hylling Sørensen, Julio Xavier Vianna Neto, Mark Kelly, Torben Krogh Mikkelsen, and Gunner Christian Larsen. Power curve and wake analyses of the Vestas multi-rotor demonstrator. *Wind Energy Science*, 4(2):251–271, may 2019.
- [36] Gunner C Larsen, Helge Aa Madsen, J Torben, and Niels Troldborg. Wake modeling and simulation. Technical Report July, Risø National Laboratory for Sustainable Energy, Risø R-1653(EN), 2008.
- [37] Pablo S. González Cisneros and Herbert Werner. Nonlinear model predictive control for models in quasi-linear parameter varying form. *International Journal of Robust and Non-linear Control*, 30(10):3945–3959, 2020.
- [38] Christian Bak, Frederik Zahle, Robert Bitsche, and Taeseong Kim. The DTU 10-MW reference wind turbine. In *Danish Wind Power Research 2013*, Fredericia, Denmark, 2013.
- [39] Anand Natarajan, Andreas Knauer, Ervin Bossanyi, Gunner Chr Larsen, Ishaan Sood, Mantthieu Irondele, Nikolay Dimitrov, and Renzo Ruisi. Advanced integrated supervisory and wind turbine control for optimal operation of large Wind Power Plants. Technical report, 2021.
- [40] Christian Bak, Frederik Zahle, Robert Bitsche, Taeseong Kim, Anders Yde, Lars Christian Henriksen, Morten Hartvig Hansen, José Pedro Albergaria Amaral Blasques, Mac Gaunaa, and Anand Natarajan. The dtu 10-mw reference wind turbine, 2013.
- [41] Jay P. Goit and Johan Meyers. Optimal control of energy extraction in wind-farm boundary layers. *Journal of Fluid Mechanics*, 768:5–50, 2015.
- [42] Dries Allaerts and Johan Meyers. Gravity Waves and Wind-Farm Efficiency in Neutral and Stable Conditions. *Boundary-Layer Meteorology*, 166(2):269–299, 2018.
- [43] Wim Munters and Johan Meyers. Effect of wind turbine response time on optimal dynamic induction control of wind farms. *Journal of Physics: Conference Series*, 753:052007, 2016.
- [44] Ishaan Sood and Johan Meyers. Reference Windfarm database PDK 0, February 2020.
- [45] Ishaan Sood and Johan Meyers. Reference Windfarm database PDK 90, February 2020.
- [46] Ishaan Sood and Johan Meyers. Reference Windfarm database CNk2 30, February 2020.
- [47] Ishaan Sood and Johan Meyers. Reference Windfarm database CNk2 60, February 2020.
- [48] Ishaan Sood and Johan Meyers. Reference Windfarm database CNk4 30, February 2020.
- [49] Ishaan Sood and Johan Meyers. Reference Windfarm database CNk4 90, February 2020.
- [50] Marc Calaf, Charles Meneveau, and Johan Meyers. Large eddy simulation study of fully developed wind-turbine array boundary layers. *Physics of Fluids*, 22(1):015110, 2010.
- [51] Dries Allaerts and Johan Meyers. Large eddy simulation of a large wind-turbine array in a conventionally neutral atmospheric boundary layer. *Physics of Fluids*, 27(6), 2015.
- [52] Wim Munters and Johan Meyers. Optimal dynamic induction and yaw control of wind farms : effects of turbine spacing and layout Optimal dynamic induction and yaw control of wind farms : effects of turbine spacing and layout. 2018.

- [53] Athanasios Vitsas and Johan Meyers. Multiscale aeroelastic simulations of large wind farms in the atmospheric boundary layer. *Journal of Physics: Conference Series*, 753(8):082020, sep 2016.
- [54] Luca Lanzilao and Johan Meyers. A new wake-merging method for wind-farm power prediction in the presence of heterogeneous background velocity fields. *Wind Energy*, 25:237–259, 07 2021.
- [55] Majid Bastankhah and Fernando Porté-Agel. Experimental and theoretical study of wind turbine wakes in yawed conditions. *Journal of Fluid Mechanics*, 806:506–541, 2016.
- [56] Haohua Zong and Fernando Porté-Agel. A momentum-conserving wake superposition method for wind farm power prediction. *Journal of Fluid Mechanics*, 889:A8, 2020.
- [57] Holoborodko Pavel. Cubature formulas for the unit disk, 2011.
- [58] Ishaan Sood, Wim Munters, and Johan Meyers. Effect of conventionally neutral boundary layer height on turbine performance and wake mixing in offshore windfarms. *Journal of Physics: Conference Series*, 1618(6), 2020.
- [59] Wessel N. van Wieringen. Lecture notes on ridge regression. 2015.
- [60] Pauli Virtanen, Ralf Gommers, Travis E. Oliphant, Matt Haberland, Tyler Reddy, David Cournapeau, Evgeni Burovski, Pearu Peterson, Warren Weckesser, Jonathan Bright, Stéfan J. van der Walt, Matthew Brett, Joshua Wilson, K. Jarrod Millman, Nikolay Mayorov, Andrew R. J. Nelson, Eric Jones, Robert Kern, Eric Larson, C J Carey, İlhan Polat, Yu Feng, Eric W. Moore, Jake VanderPlas, Denis Laxalde, Josef Perktold, Robert Cimrman, Ian Henriksen, E. A. Quintero, Charles R. Harris, Anne M. Archibald, Antônio H. Ribeiro, Fabian Pedregosa, Paul van Mulbregt, and SciPy 1.0 Contributors. SciPy 1.0: Fundamental Algorithms for Scientific Computing in Python. *Nature Methods*, 17:261–272, 2020.
- [61] Bart M. Doekemeijer, Daan van der Hoek, and Jan Willem van Wingerden. Closed-loop model-based wind farm control using FLORIS under time-varying inflow conditions. *Renewable Energy*, 156:719–730, 2020.
- [62] Ishaan Sood and Johan Meyers. Validation of an analytical optimization framework for wind farm wake steering applications. *AIAA SCITECH 2022 Forum*.
- [63] K. Kölle, T. Göçmen, I. Eguinoa, L. A. Alcayaga Román, M. Aparicio-Sanchez, J. Feng, J. Meyers, V. Pettas, and I. Sood. Farmconners market showcases results: Wind farm flow control considering electricity prices and revenue. *Wind Energy Science Discussions*, 2022:1–29, 2022.
- [64] Ishaan Sood and Johan Meyers. Tuning of an engineering wind farm model using measurements from Large Eddy Simulations. *Journal of Physics: Conference Series*, ((accepted)), 2022.
- [65] Herbert J Sutherland. On the Fatigue Analysis of Wind Turbines. Technical report, Sandia National Laboratories (SNL), Albuquerque, NM, and Livermore, CA, 1999.
- [66] D.F. Socie and S.D. Downing. Simple Rainflow Counting Algorithms. *International Journal of Fatigue*, 4(1):31–40, 1982.